94CH3445-4

THE INSTITUTE OF ELECTRICAL
AND ELECTRONICS ENGINEERS, INC.

IEEE

Conference Record of the 1994 IEEE International Symposium on Electrical Insulation

Sheraton Station Square Hotel
Pittsburgh, Pennsylvania
June 5-8, 1994

Sponsored by the IEEE

DIELECTRICS AND ELECTRICAL
INSULATION SOCIETY

Printed in Canada

Conference Record of the 1994 IEEE International Symposium on Electrical Insulation, Pittsburgh, PA USA, June 5-8, 1994

PERFORMANCE EVALUATION OF A NEW DIGITAL PARTIAL DISCHARGE RECORDING AND ANALYSIS SYSTEM

P. von Glahn* and R. J. Van Brunt
National Institute of Standards and Technology
Gaithersburg, MD 20899

Abstract

We describe the design and performance evaluation of a new digital partial discharge (PD) recording system capable of real-time recording of PD pulse trains for later off-line computerized stochastic analysis. The new recording system consists of a custom two-channel PD digitizer coupled to a new 16-bit parallel digital interface installed in a personal computer. The digitizer is under software control with the resulting data being stored in binary files on the computer's hard disk. Since post-test analysis software run on the computer provides the needed stochastic analysis of the data files, the new system offers a unique capability to perform stochastic analysis on non-stationary PD data such as found in aging studies. By way of illustration, measurements were made of the time-varying stochastic behavior of ac-generated PDs in point-to-dielectric gaps in air where the insulation material was cast epoxy with aluminum oxide filler, extending the work reported previously. Sample analysis results are presented, demonstrating that the new system provides analysis results comparable with the results achieved by the existing NIST analog PD stochastic analysis system. Sample stochastic analysis results are presented demonstrating the additional insights possible with the new system.

Introduction

With the advent of high-speed digital logic and computers, it was natural to apply these to the measurement of partial discharge signals. By the mid 1970s, a number of authors had reported using digital processors to acquire and process PD signals in real time, mostly in the form of pulse-height analysis [1-3]. By the late 1980s, computer processing of PD data to determine phase-resolved PD signatures had supplanted the earlier analysis techniques [4-5]. Coupling a high-speed personal computer with custom digital data acquisition system for real-time recording and post-test PD analysis using both phase-resolved PD signatures and neural networks was a logical next step in the development of digital PD analysis technology [6-8]. In the early 1990s, Van Brunt recognized that PD is a non-Markovian point process, requiring more sophisticated analyses to understand the physical basis of the phenomenon than could be accomplished with existing PD measurement systems [9]. This led to the development of a sophisticated real-time analog PD stochastic analyzer [10]. Van Brunt's analyzer allowed direct measurement of various conditional PD phase and amplitude distributions which can be used to gain new insights into PD behavior.

The present work documents a new digitizer with attendant analysis software capable of recording PD signals in real time and performing a complete stochastic analysis of the recorded data. For purposes of illustration, we present data on PD-induced aging of epoxy discussed in our previous work [11-12]. In the following section, the architecture and operation of the new digitizating and recording systems are described. After a description of the experimental configuration, a comparison is made between data recorded simultaneously with the new digital system and the older analog analyzer. The results of several new types of analysis are presented demonstrating typical results obtainable with the new system.

* Faculty member, Dept. of Physics and Astronomy, Delaware State University, Dover, DE 19901.

Digitizer Description

The PD Digitizer and Recording System (PDRS) consists of two parts: a digitizer connected to an interface card installed in an expansion slot in a personal computer (PC). The PDRS digitizes a PD pulse stream as a series of 16-bit words which are recorded on the PC's hard disk. The polarity, amplitude and time since the last positive-going zero-crossing of the applied alternating voltage are recorded for each pulse. A word corresponding to each zero-crossing is also recorded. A 5-bit record number included within the amplitude and zero-crossing words allows multiple records to be stored within one data file; the record number is loaded into the digitizer by software in the PC. Figure 1 shows two consecutive, randomly-selected, cycles of PD data reconstructed from the digitized information given in Table I. Table I

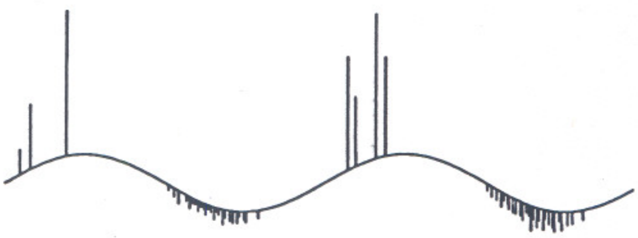

Figure 1. Sample PD signal for two successive, randomly-selected, cycles of applied voltage.

Table I. Sample digitizer data corresponding to Fig. 1 in hexadecimal notation. First column is address within data file. Zero-crossings underlined

000100:	440c	2108	<u>61ff</u>	403c	0112	4065	0134	40f3
000110:	0174	4282	2109	4296	2115	42a8	2128	42c7
000120:	210e	42d3	2124	42de	210c	42e9	210c	42f4
000130:	2121	42ff	210c	430b	210e	4310	2122	431c
000140:	210a	4326	2112	4332	212a	433b	2109	4344
000150:	2113	4355	2135	435e	2118	4370	2121	437e
000160:	2127	438d	2126	4395	210b	43a5	2116	43ad
000170:	2122	43df	2113	<u>61ff</u>	405c	013b	4078	0123
000180:	40c9	014c	40ed	0133	4277	2105	4287	210e
000190:	429a	210f	42ad	211b	42b7	2108	42c5	210a
0001a0:	42ca	2116	42da	211b	42e5	211b	42f8	211a
0001b0:	4300	2122	430d	210e	4316	2112	4320	2136
0001c0:	432c	2118	4338	2128	4341	2115	4350	212a
0001d0:	4357	210c	4367	211a	4375	211f	437c	212a
0001e0:	438e	210e	4399	2125	43b0	2116	43c4	2114
0001f0:	43ec	210c	<u>61ff</u>	4059	0139	40ac	0157	40d7

Table II. Digitizer recorded data format in binary and hexadecimal notation. (rrrrr: 5-bit record number; a...a: 8-bit pulse amplitude; p...p: 13-bit pulse phase; x...x: random data)

Binary	Hexadecimal	Meaning
000rrrrr aaaaaaaa	0raa - 1raa	Positive pulse amplitude
001rrrrr aaaaaaaa	2raa - 3raa	Negative pulse amplitude
010ppppp pppppppp	4ppp - 5ppp	Phase
011rrrrr xxxxxxxx	6rxx - 7rxx	Zero-crossing marker

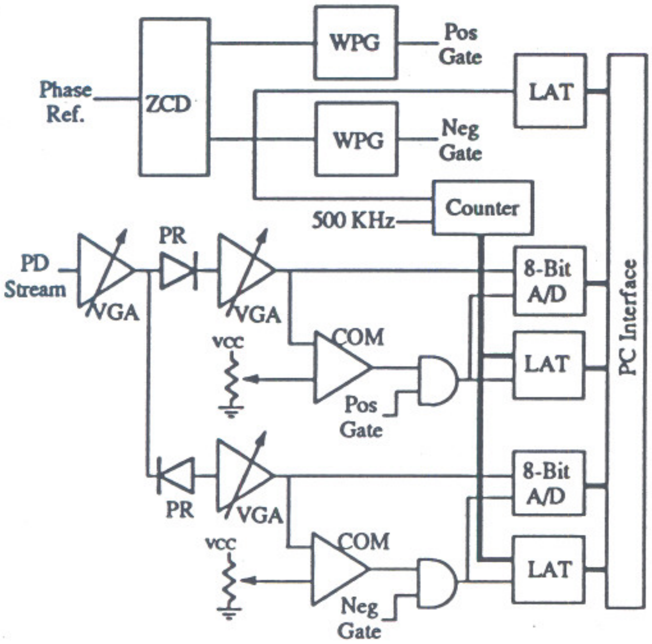

Figure 2. Block diagram of digitizer (A/D: Analog to digital converter, COM: Analog voltage comparator, LAT: Digital latch, PR: Precision Rectifier, VGA: Variable gain amplifier, WPG: Window pulse generator, ZCD: Zero Crossing Detector)

defines the corresponding data storage format.

The digitizer, shown in Fig. 2, is similar to that reported in [7-8]. It is connected to a custom 16-bit interface card in the PC (not shown). The custom interface provides rate buffering and temporary storage of digitizer data prior to processing by the PC. The digitizer is under the control of software running on the PC and consists of two sections: a timing generator and a two-channel digitizer.

The timing generator section is based on a phase reference signal derived from the AC excitation source by external circuitry. A zero-crossing detector generates signals from the reference signal at both the positive- and negative-going zero-crossings of the reference signal. The positive-going zero-crossing pulse causes the zero-crossing word to be transferred to the PC. It also resets the pulse time counter and triggers variable window pulse generator which generates a gate for negative PD pulses. The negative-going pulse likewise triggers a second window pulse generator to provide a gate for positive PD pulses. The two window pulses generators are manually adjusted so that the gates cover the phase range where positive (negative) pulses are observed. Note that PD pulses immediately prior to the positive-going zero-crossing will be stored with the cycle prior to the zero-crossing; analysis software associates these "late" pulses with the correct cycle.

The digitizer section is preceded by an analog signal conditioner. The analog conditioner accepts a stream of bipolar PD pulses from a capacitively-coupled preamplifier that broadens the pulses to 1.5 μs (half-width). After an initial amplification, the PD stream is fed to a pair of precision rectifiers (half-wave rectifiers implemented with operational amplifiers and diodes) to break the PD stream into separate positive and negative pulse streams. Further amplification follows the rectifiers to bring the pulses within the range of the analog-to-digital (A/D) converters. The digitizer section consists of two identical circuits, one for each pulse polarity. The PD pulse is digitized by an 8-Bit peak-detecting A/D converter that stores the largest input amplitude detected while it is enabled. The PD pulses are also fed to a voltage comparator. When the pulse amplitude exceeds a user-defined voltage threshold, the comparator output becomes active. If the PD pulse falls within the window generated by the pulse generator, the current value of the pulse time counter is latched. The time counter is clocked by a 500 KHz signal, so the phase resolution of the digitizer is 2.4×10^{-4} rad (at 60 Hz). After a 1 μs delay to allow the PD signal to reach its peak value, the A/D converter is deactivated and the resulting amplitude and phase data are transferred to the PC for recording. The transfer process is completed in 2.5 μs from the activation of the comparator output which defines the minimum inter-pulse resolution time of the instrument.

Experimental Configuration

The experimental results reported below were obtained from an alternating voltage applied to a point-dielectric gap using the same epoxy dielectric samples and configuration reported in [11-12]. In the case where the point electrode touched the epoxy surface, it was found that the positive PD pulses eventually ceased due to a PD-induced increase in surface conductivity. As shown in Fig. 3, the PD pulse stream was amplified by a dual-output preamplifier and processed in parallel by the PDRS and the Analog Stochastic Analyzer (ASA) described elsewhere [10,13]. The ASA was configured to simultaneously generate three types of outputs: positive pulse amplitude integrated over one cycle, negative pulse amplitude integrated over one cycle, and the phase of the first negative pulse. Each output was digitized using a separate Multi-Channel Analyzer (MCA) and recorded on disk files on a personal computer.

The ASA was operated for two 50-second periods during the experiment, one immediately upon power application and one near the point of positive pulse termination. The PDRS was used to collect data for eight one-minute periods from power application until two minutes after the positive pulses ceased. Time intervals of 11 and 34 seconds separated successive recordings. Data for each period were stored in a separate disk file, resulting in 13.1 megabytes of binary data files.

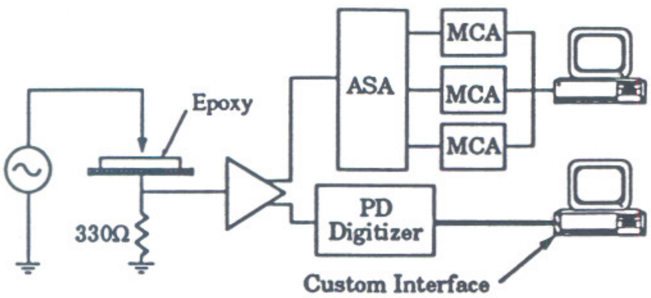

Figure 3. Experiment configuration block diagram. Material: Epidian Type 2 Epoxy† with Al_2O_3 Filler, Needle-insulator distance: 0 cm, Sinusoidal excitation: 3 KV, 400 Hz. (ASA: Analog Stochastic Analyzer, MCA: Multi-Channel Analyzer)

The ASA outputs were calibrated using the procedure described in [10]. The PDRS amplitude measurements were calibrated using a pulse signal applied to a known capacitor connected in place of the point-dielectric gap in Figure 3. The pulse generator was synchronized to the AC excitation frequency and the pulse width was adjusted so that transitions generating impluses corresponding to positive and negative PD signals were within the positive and negative gates, respectively. A digital file was recorded containing data records for different calibration pulse amplitudes ranging from an amplitude that saturated the positive digitizer to a level that generated only a few counts on the negative digitizer. The resulting data file was used to convert the recorded pulse amplitudes into units of charge (pC).

Custom software executing on a PC was used to analyze the stored data. In the case of the ASA data files, the analysis consisted of reading the stored MCA histogram data and using calibration data to convert the histogram index (i.e., horizontal axis) to phase or charge (e.g., rad or pC). For the PDRS, more extensive software is needed to read and decode the digitized data format, calibrate amplitudes and phases, and perform the required stochastic analysis.

Experimental Results

Figure 4 shows a comparison of data on integrated charge distributions ($p_0(Q^+)$, $p_0(Q^-)$) and phase-of-occurrence of the first negative pulse ($p_0(\phi_1)$) where Q^+ and Q^- are the sums of PD pulse amplitudes on the positive and negative cycles, respectively. As can be seen from Fig. 4, the results generated by the two analysis approaches are similar. Note that, due to threshold limits of the ASA, the PDRS results give data at lower amplitudes as well as for a broader range of phase angles than the results from the ASA. The large peak at zero charge on the $p_0(Q^+)$ plot indicates that a significant number of cycles with no positive pulses occur during the first 50 seconds of PD operation, a fact that cannot be determined from the ASA data. The source of the small peak

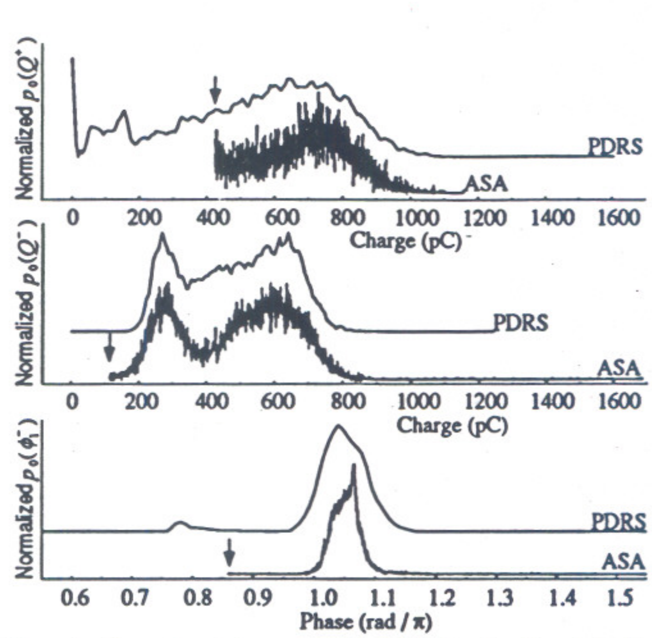

Figure 4. Comparison between normalized PDRS and analog stochastic analyzer data for 50 s after power application. Plots show positive pulse integrated charge, negative pulse integrated charge, and phase-of-occurrence of first negative pulse. Vertical arrows indicate ASA threshold setting.

on the PRDS $p_0(\phi_1)$ plot at approximately 0.78 rad / π cannot be explained at the present time.

The same PDRS data can be analyzed for different time intervals to extract information about the time dependence of the stochastic behavior The following figures were all generated by analyzing the same 8 data files using 20-second processing windows.

Figures 5, 6, and 7 give a time history of the three distributions shown in Fig. 4. They show the same trends associated with the aging of epoxy previously reported using ASA data [9,10].

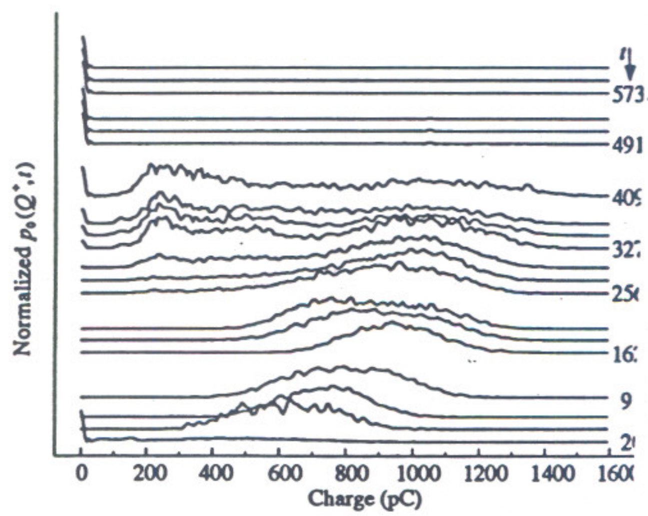

Figure 5. Normalized positive pulse integrated charge vs time in seconds (20 s integration window)

†Certain commercial materials are identified in this paper to specify adequately the experimental procedure. Such identification does not imply recommendation or endorsement by the National Institute of Standards and Technology, nor does it imply that the materials identified are necessarily the best available for the purpose.

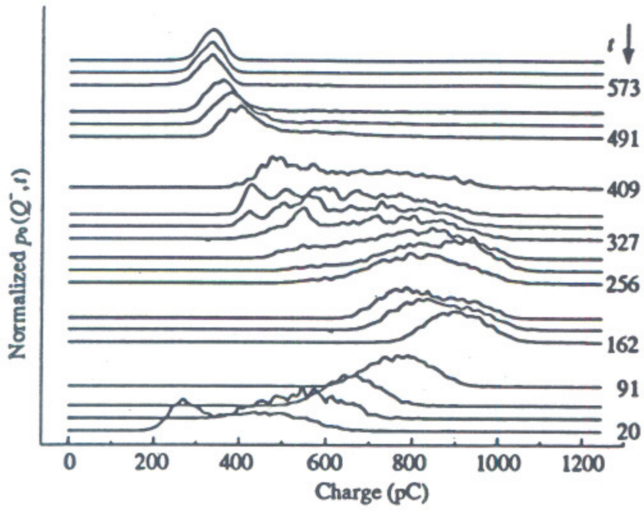

Figure 6. Normalized negative pulse integrated charge vs time in seconds. (20 s integration window)

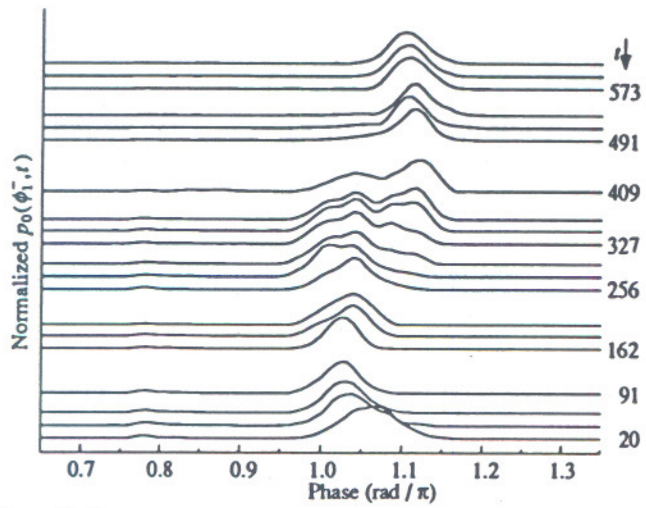

Figure 7. Normalized phase-of-occurrence of first negative pulse *vs* time in seconds. (20 s processing window)

Additional information about the aging process is provided by behavior of the mean number $(\langle n^+\rangle, \langle n^-\rangle)$ and mean amplitude $(\langle q^+\rangle, \langle q^-\rangle)$ of pulses over time as shown in Figures 8 and 9. The vertical bars on these plots give the maximum and minimum values recorded on any cycle during the 20-second processing window. The curves correspond to mean values determined by averaging the data from all cycles during the same processing period.

Figure 8 shows that even when the average number of positive pulses tends toward zero, some cycles do occur with one or more pulses. It also shows that during the time when positive PD pulses regularly occur, at least one cycle in many of the processing windows had no positive pulses.

Figure 9 illustrates one limitation of the current PDRS, namely its lack of dynamic range. A significant number of

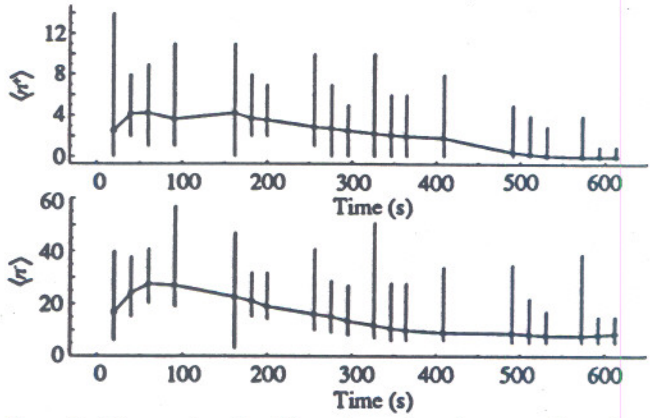

Figure 8. Mean number of positive and pegative pulses per cycle *vs* time. Vertical bars connect maximum and minimum pulse count within 20 s processing window

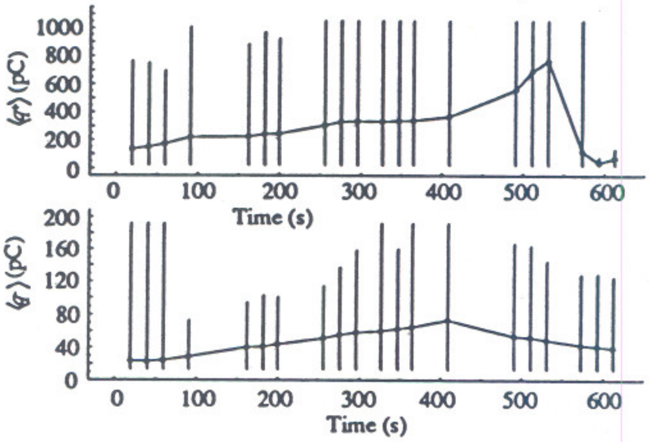

Figure 9. Mean positive and negative pulse amplitude *vs* time. Vertical bars connect maximum and minimum pulse amplitudes within 20 s processing window.

positive and negative processing windows show maximum amplitudes corresponding to saturation of the A/D converter. Note also that for every processing period there exists at least one cycle with no pulses above the minimum of the A/D converter. These "zero-height" pulses occur when the analog comparator threshold setting is below the A/D minimum input level and introduce errors in both the number of pulses and average pulse amplitude data.

Conclusions

We have shown that the PDRS can produce results that compare favorably with those of the proven real-time PD analysis system. Further, the PDRS provides an ease of calibration and the ability to make new types of analyses which are impossible with a real-time system, such as the distribution in number of PD pulses per cycle. More importantly, the PDRS can produce archival records of all PD activity providing a new opportunity not only to make multiple analyses of the same segment of data but also to re-analyze the data in the future in the light of new understanding of the PD phenomena or for comparison with later records from the same apparatus.

The present PDRS design is limited to recording PD pulses with an impulsive shape with a separation of at least 2.5 μs. It will produce inaccurate results for PD streams containing bursts of closely-spaced pulses [14-15] or pulses with long "tails" [16]. It also requires a PC with a fast processor and large hard disk to keep up with and store the PD stream. Finally, in its current configuration, it lacks sufficient dynamic range to accurately track PD signals with large fluctuations in amplitude while maintaining calibration.

Areas for Future Work

Additional work is planned to further validate the performance of the PDRS through comparison with the ASA. The dynamic range limitations will be addressed through the addition of calibrated, digital gain and threshold settings to replace the current analog controls and allow the system to dynamically track signal levels. Finally, the analysis software is continually being upgraded to take advantage of the new types of analysis made possible by the PDRS so as to gain new understanding into the physics of the PD phenomena and move toward the day when reliable computerized life predictions of high voltage apparatus based on PD signals is a reality.

Acknowledgments

All measurements were made in the Electricity Division, Electronics and Electrical Engineering Laboratory, National Institute of Standards and Technology, Technology Administration of the US. Department of Commerce. The epoxy samples used were provided by T. Las of the Electrotechnical Institute, Warsaw, Poland.

References

[1] R. Bartnikas, "Use of a Multichannel Analyzer for Corona Pulse-Height Distribution Measurements on Cables and Other Electrical Apparatus," IEEE Trans. Instru. Meas., IM-22, 403-407, (1973).

[2] T. Tanaka and T. Okamoto, "A Minicomputer-Based Partial Discharge Measurement System," Conf. Recd. 1978 IEEE Intl. Symp. Elect. Insul, pp. 86-89.

[3] J. Austin and R. James, "On-Line Digital Computer Systems for Measurement of Partial Discharges in Insulation Structures," IEEE Trans. Elect. Insul., EI-11, 129-139 (1976).

[4] B. Fruth, L. Neimeyer, M. Häsig, J. Fuhr, and Th. Dunz, "Phase Resolved Partial Discharge Measurements and Computer Aided Partial Discharge Analysis Performed on Different High Voltage Apparatus," 6th Intl. Symp. HV Eng'g., New Orleans, pp. 15.03-15.06 (1989).

[5] M. Hikita, et.al., "Measurements of Partial Discharges b Computer and Analysis of Partial Discharge Distribution b the Monte Carlo Method," IEEE Trans. Elect. Insul. 25, 453 468 (1990).

[6] T.R. Blackburn, B.T. Phung, and R.E. James, "Neura Network Application of PD Pattern Analysis," Conf. Proc Intl. Conf. Partial Discharge, Canterbury, UK, pp. 82-8 (1993).

[7] C. Hantouche and D. Fortune, "Digital Measurement o Partial Discharges in Full-sized Power Capacitors," IEEI Trans. Elect. Insul. 28, 1025-1032 (1993).

8] R.E. James, B.T. Phung and T.R. Blackburn, "Computer-Aided Digital Techniques for Partial Discharge Measurements and Analysis," Intl. Symp. Digital Techn High-Volt. Meas., Toronto, Canada, pp. 2.7-2.11 (1991).

[9] R.J. Van Brunt, "Stochastic Properties of Partial-Discharge Phenomena," IEEE Trans. Elect. Insul 26, 902-948 (1991).

[10] R.J. Van Brunt and E.W. Cernyar, "System for Measuring Conditional Amplitude, Phase, or Time Distributions of Pulsating Phenomena," J. Research of Natl. Inst. Std. Techn. 97, 634-671 (1992).

[11] R.J. Van Brunt and P. von Glahn, "Nonstationary Behavior of Partial Discharge During Insulation Aging," Conf. Proc. Intl. Conf. Partial Discharge, Canterbury, UK, pp. 29-30 (1993).

[12] R.J. Van Brunt, P. von Glahn, and T. Las, "Partial Discharge-Induced Aging of Cast Epoxies and Related Nonstationary Behavior of the Discharge Statistics," 1993 Annual Report, Conference on Electrical Insulation and Dielectric Phenomena, Pocono Manor, PA, pp. 455-461.

[13] R.J. Van Brunt, E.W. Cernyar, and P. von Glahn, "Importance of Unraveling Memory Propagation Effects in Interpreting Data on Partial Discharge Statistics," IEEE Trans. Elect. Insul. 28, 905-916 (1993).

[14] R.J. Van Brunt and D. Leep, "Characterization of Point-to-Plane Corona Pulses in SF6," J. Appl. Phys. 52, 658-600 (1981).

[15] T.V. Blalock, A.L. Wintenberg, and M.O. Pace, "Low Noise- Wide-Band Amplification System for Acquiring Prebreakdown Current Pulses in Liquid Dielectrics," IEEE Trans. Elect. Insul. 24, 641-647 (1989).

[16] R. Bartnikas and J.P. Novak, "On the Character of Different Forms of Partial Discharge and Their Related Terminologies," IEEE Trans. Elect. Insul. 28, 956-968 (1993).